Available online at www.sciencedirect.com
SCIENCE DIRECT®
Journal of Molecular Catalysis B: Enzymatic 33 (2005) 35–42
JOURNAL OF MOLECULAR CATALYSIS B: ENZYMATIC
www.elsevier.com/locate/molcatb

Reaction mechanism to explain the high kinetic autoactivation of tyrosinase

Maria J. Peñalver[a], Lorena G. Fenoll[a], José N. Rodríguez-López[a], Pedro A. García-Ruiz[b], Francisco García-Molina[a], Ramón Varón[c], Francisco García-Cánovas[a,*], José Tudela[a]

[a] *GENZ: Grupo de Investigación de Enzimología, Departamento de Bioquímica y Biología Molecular-A, Facultad de Biología, Universidad de Murcia, A. Correos 4021, E-30080 Murcia, Spain*
[b] *Departamento de Química Orgánica, Facultad de Química, Universidad de Murcia, Murcia, Spain*
[c] *Departamento de Química Física, Escuela Técnica Superior de Albacete, Universidad de Castilla La-Mancha, Castilla La-Mancha, Spain*

Received 1 July 2004; received in revised form 16 February 2005; accepted 17 February 2005
Available online 28 March 2005

Abstract

The autoactivation of tyrosinase acting on monophenols has been quantitatively characterised by a new kinetic parameter, the rate autoactivation factor (RAF). This parameter is equivalent to the ratio between the initial and final steady-state rates of tyrosinase in its monophenolase activity. The experimental RAF data for L-tyrosine point to a kinetic behaviour with respect to the monophenol and enzyme concentrations, which coincides with the data obtained in numerical simulations of the kinetic reaction mechanism proposed for tyrosinase. Moreover, the experimental data are also in agreement with the expected dependencies obtained from the analytical expression of RAF, as described in this paper. These results establish the validity of the kinetic reaction mechanism proposed by us for tyrosinase, and confirm the melanogenesis pathway described in text books: tyrosine → dopa → dopaquinone → dopa + melanins → melanins.

Keywords: Lag period; Monophenol; Mushroom; Polyphenol oxidase; Tyrosine

1. Introduction

Tyrosinase or polyphenoloxidase is a copper enzyme widely distributed throughout the phylogenetic scale. It catalyses the hydroxylation of monophenols (M) to *o*-diphenols (D) and their subsequent oxidation to *o*-quinones (Q), in both cases by molecular oxygen [1,2]. The catalytic action of tyrosinase on M is possible because there is a small proportion of *oxy*tyrosinase (E_{ox}, 2–30%) in the native enzyme [3].

The kinetic behaviour of tyrosinase is very complex due to the contemporaneous occurrence of the enzymatic oxidation of M and D to Q, on the one hand, and the coupled non-enzymatic reactions of Q on the other [3,4]. The kinetic constants of these non-enzymatic reactions of Q and their dependence on pH and temperature have previously been determined by our group [5,6]. We also demonstrated the regeneration of D from Q by non-enzymatic reactions: intramolecular cyclization reactions [7,8], the addition of water [6,9] or the addition of other nucleophilic reagents [10,11].

Understanding the non-enzymatic reactions of Q led us to propose a kinetic reaction mechanism for the enzymatic oxidation of M and D to Q catalysed by tyrosinase [12,13]. We initially proposed a simple kinetic mechanism, the numerical simulation of which was in qualitative agreement with the principal experimental results obtained for tyrosinase [12]. We later proposed a more detailed kinetic mechanism and deduced the analytical expressions for the steady-state rates for the monophenolase and diphenolase activities of tyrosinase [13,14] (Scheme 1). Moreover, the effects on the enzyme's action kinetics were considered in the case of substrates which evolve by rapid cyclization, such as L-tyrosine/L-dopa [14], or by the slow addition of water, such as 4-*tert*-butylphenol/4-

* Corresponding author. Tel.: +34 968 364782; fax: +34 968 364147.
E-mail address: canovasf@um.es (F. García-Cánovas).
URL: http://www.um.es/genz.

1381-1177/$ – see front matter © 2005 Elsevier B.V. All rights reserved.
doi:10.1016/j.molcatb.2005.02.002

Nomenclature

A	auxiliary *o*-diphenol when the enzyme acts on M
Cr	aminochrome
D	*o*-diphenol
D released	D released enzymatically when the enzyme acts on M
$[D]_0$	initial concentration of D
$[D]_{ss1}$	concentration of enzymatically released D in the initial pseudo steady-state
$[D]_{ss2}$	concentration of D in the final steady-state, mainly originated by the evolution of Q
E_m	mettyrosinase
E_d	deoxytyrosinase
E_{ox}	oxytyrosinase
$[E]_0$	total concentration of enzyme
$[E_{ox}]_0$	initial concentration of enzyme in oxytyrosinase form
$[E_{ox}]_{ss1}$	concentration of oxytyrosinase in first steady-state
$[E_{ox}]_{ss2}$	concentration of oxytyrosinase in second steady-state
k^M_{cat2}	the catalytic constant for the second steady-state
K^M_{m2}	The Michaelis constant for the second steady-state
K_1	dissociation constant of E_mM complex ($K_1 = k_{-1}/k_1$)
K_2	dissociation constant of E_mD complex ($K_2 = k_{-2}/k_2$)
M	monophenol
$[M]_0$	initial concentration of M
Q	*o*-quinone
R_{ox1}	ratio between the concentration of oxytyrosinase in the first steady-state and the total concentration of enzyme ($R_{ox1} = [E_{ox}]_{ss1}/[E]_0$)
RAF^M	rate autoactivation factor in the action of tyrosinase on monophenols. Same as the ratio between the velocity of the final steady-state (V^M_{ss2}) and the velocity of the initial steady state (V^M_{ss1}). $RAF^M = V^M_{ss2}/V^M_{ss1}$
Tyr	L-tyrosine
V^M_{ss1}	first steady-state rate of monophenolase activity of tyrosinase
V^M_{ss2}	final steady-state rate of monophenolase activity of tyrosinase
V^{Tyr}_{ss1}	initial steady-state rate when tyrosinase acts L-tyrosine
V^{Tyr}_{ss2}	final steady-state rate when tyrosinase acts L-tyrosine
τ	lag period

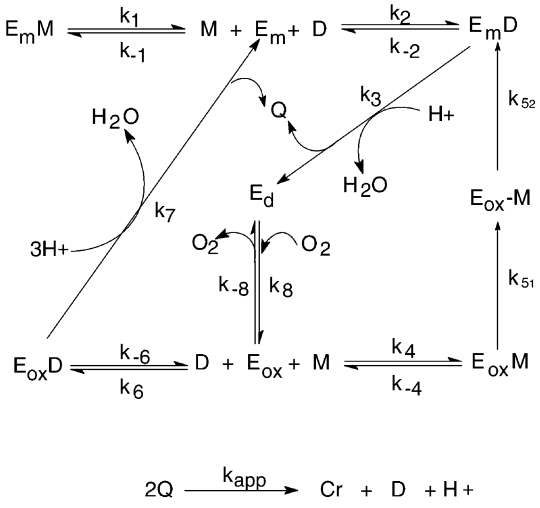

Scheme 1. Propose kinetic reaction mechanism of tyrosinase acting on M and D, with the non-enzymatic reactions corresponding the evolution of Q. E_d is converted to E_{ox} by binding oxygen (O_2). E_{ox} can either react with a monophenol, M or with an *o*-diphenol, D. In the case of E_{ox} reacting with M, this evolves to D and may be oxidised to Q, generating E_d, or be released into the medium, generating, in turn, E_m. If E_{ox} reacts with D, the corresponding Q is generated. E_m can oxidise D, generating Q, and be converted to E_d, and E_m may bind to M generating the dead-end complex, E_mM. Spontaneous endocyclization of Q gives rise to dopachrome (Cr) and D. Mechanism previously proposed by us [13].

tert-butylcatechol [15]. All these data were compiled in a review [16].

The validity of the kinetic reaction mechanism proposed for tyrosinase [13], has been substantiated for enzymes extracted from a variety of fruit and vegetables [17,18]. Moreover, the stereospecificity of tyrosinase from several sources has been studied [18–20] and, using stopped-flow techniques, the rate constant for the O_2 binding to E_d (*deoxy*tyrosinase) (k_8), has been determined [21] (Scheme 1).

It has recently been demonstrated that the transformation of $E_{ox}M$ (*oxy*tyrosinase monophenol binding complex) into E_mD (*met*tyrosinase diphenol binding complex) and E_mM (*met*tyrosinase monophenol binding complex), with the release of D (Scheme 1), during the enzymatic formation of Q from M contributes to the initial steady-state of tyrosinase [22,23], while the regeneration of D in non-enzymatic reactions from Q [5,7,13] contributes to the final steady-state of tyrosinase [22,23]. Using gas chromatography/mass spectrometry, it has been demonstrated that D is released during the enzymatic oxidation of M to Q [24], and that the quantity of D released increases in the presence of an auxiliary *o*-diphenol (A) [24]. These experimental results support the validity of the kinetic reaction mechanism proposed for tyrosinase [13] (Scheme 1), since they confirm the enzymatic release of D from the tyrosinase reaction with M, in addition to the non-enzymatic regeneration of D from Q.

On the other hand, some authors have proposed another kinetic reaction mechanism for tyrosinase [25,26] (Scheme 2) which is really a simplification of our reaction mechanism [13] (Scheme 1). These authors have published numerical

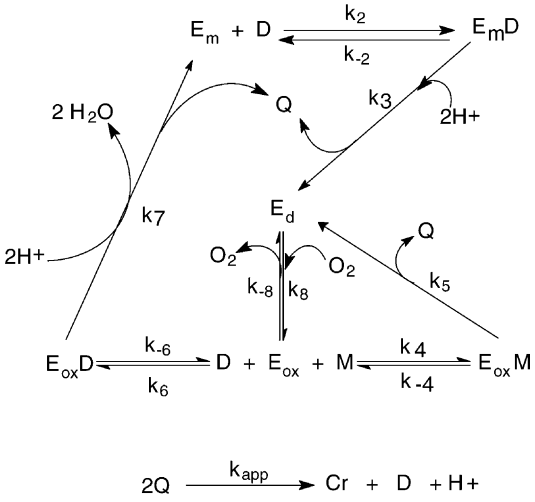

Scheme 2. Kinetic reaction mechanism of tyrosinase acting on M and D, with the non-enzymatic reactions corresponding to the Q evolution. E_d is converted to E_{ox} by binding O_2. E_{ox} can either react with M or with D to give the corresponding Q. E_m can oxidize D, generating Q, and be converted to E_d. Spontaneous endocyclization of Q gives rise to Cr and D. No steps describing the transformation of $E_{ox}M$ to E_mD or of E_m to E_mM are included. Mechanism previously proposed by other authors [25,26,32].

simulations of their mechanism [26] but have deduced no analytical expression for its steady-state rate. Recently, other authors have conceptually criticised the inconsistency of Mechanism II [26], arguing that it does not satisfactorily explain a wide variety of data obtained experimentally for tyrosinase, at least up to 1999 [27].

Our group, in a recent publication [28], included new experimental data on the kinetic behaviour of tyrosinase, which was compared with new numerical simulations of Mechanism I [13] and II [26]. This work [28] described our most recent kinetic studies on tyrosinase [21–24,29–31] emphasizing the importance of the chemical reactions generated from Q and the analytical expressions of the steady-state rate equations [13,14].

The above work [28], which focused on critical experiments, helped to discriminate between the feasibility of each mechanism. Thus, the following were considered: variation of τ (lag period) versus $[M]_0$, variation of V_{ss1}^{M} (the first steady-state rate) versus $[M]_0$, variation of $[D]_{ss1}$ (concentration in the *pseudo* steady-state of enzymatically released D) versus $[M]_0$, variation of $[D]_{ss1}$ versus $[E]_0$ and variation of $[D]_{ss1}$ versus $[A]_0$ (auxiliary *o*-diphenol concentration when the enzyme acts on M). The conclusion reached was that the experimental data agreed with the simulation of Mechanism I but not with Mechanism II.The melanogenesis pathway described in text books:

$$\text{tyrosine} \xrightarrow{\text{tyrosinase}} \text{dopa} \xrightarrow{\text{tyrosinase}} \text{dopaquinone} \rightarrow \text{dopa} + \text{melanins} \rightarrow \text{melanins} \quad (1)$$

is supported by our reaction mechanism (Scheme 1). Recently [32], it has been proposed that the text books are mistaken and that another melanin biosynthesis pathway should be inserted:

$$\text{tyrosine} \xrightarrow{\text{tyrosinase}} \text{dopaquinone} \rightarrow \text{dopa} + \text{melanins} \rightarrow \text{melanins} \quad (2)$$

based on an alternative reaction mechanism (Scheme 2). It was also indicated that the validity of this mechanism is apparently supported by its qualitative description of the autoactivation of tyrosinase, or by the increased rate after the lag period in the oxidation of M [32].

The object of this article is to quantitatively characterise tyrosinase autoactivation by a new kinetic parameter, the rate autoactivation factor (RAF). This parameter is equivalent to the ratio between the final steady-state (V_{ss2}^{M}) and the initial steady-state (V_{ss1}^{M}) rates of tyrosinase [23] during its catalytic activity on a particular M ($\text{RAF}^{M} = \frac{V_{ss2}^{M}}{V_{ss1}^{M}}$). We shall study, the oxidation of L-tyrosine (Tyr) catalysed by tyrosinase, thus obtaining experimental data of RAF^{Tyr}, which will be contrasted with the numerical simulations of both reaction mechanisms (Schemes 1 and 2). The results will support the validity of one or other of the reaction mechanisms proposed for tyrosinase (Scheme 1 or Scheme 2) and identify the correct melanin biosynthesis pathway which should appear in the text books [32] Eqs. (1) or (2).

2. Materials and methods

2.1. Reagents

L-tyrosine was purchased from Sigma (Madrid, Spain). Stock solutions of the phenolic substrate was prepared in 0.15 mM phosphoric acid to prevent autoxidation. Milli-Q system (Millipore Corp., Spain) ultrapure water was used throughout this research. The monophenol was purified of possible contamination by the corresponding *o*-diphenol by passing them through a column 1 cm in diameter containing 2 g of aluminium oxide suspended in 0.5 M ammonium acetate pH 6.1 [33]. This solutions were further purified by Chelex-100 chromatography (100–200 mesh, Na^+ form, Bio-Rad) to remove traces of metal ions.

2.2. Enzyme source

Mushroom tyrosinase (3000 U/mg) was purchased from Sigma (Madrid, Spain) and purified by Duckworth and Coleman's procedure [34]. The enzyme concentration was calculated taking the value of M_r as 120,000. Protein content was determined by Bradford's method [35] using bovine serum albumin as standard.

2.3. Spectrophotometric assays

Absorption spectra with a 60 nm/s scanning speed were recorded in an UV–vis Perkin-Elmer Lambda-2 spectropho-

tometer, on-line interfaced with a compatible PC 486DX microcomputer and controlled with the Perkin-Elmer UVWIN-LAB software. Temperature was controlled at 25 °C using a Haake D1G circulating water-bath with a heater/cooler and checked using a Cole-Parmer digital thermometer with a precision of ±0.1 °C. Kinetic assays were also carried out with the above instruments by measuring the appearance of the products in the reaction medium. Reference cuvettes contained all the components except the substrate, with a final volume of 1 ml. All the assays were carried out under conditions of tyrosinase saturation by molecular oxygen (0.26 mM in the assay medium) [36]. The reactions were followed at a wavelength corresponding to the isosbestic point between the *o*-quinone and its corresponding aminochrome, with $\lambda_i = 410$ nm and $\varepsilon_i = 1819\ M^{-1}\ cm^{-1}$.

2.4. Kinetic analysis

The kinetic analysis of the reaction mechanisms here proposed for the action of tyrosinase on L-tyrosine led to the derivation of their corresponding analytical expressions for the first pseudo-steady-state rate V_{ss1}^{M} and for the second steady-state rate V_{ss2}^{M}, respectively. These expressions were obtained using a computer program [37,38] developed from a previously reported matrix method [39].

2.5. Simulation assays

The simulation revealed the kinetic behaviour of the concentrations of the ligand and enzymatic species involved in the reaction mechanisms here proposed for tyrosinase. The respective systems of differential equations have been solved numerically for particular sets of values of the rate constants and of initial concentrations of the species of the reaction mechanism [40]. The numerical integration is based on the Runge–Kutta–Fehlberg algorithm [41], implemented on a PC-compatible computer program (WES) [42].

2.6. Determination of the steady-state rates

The formation rate of [QH]+[Cr] in the first pseudo-steady-state, V_{ss1}^{M}, and the second steady-state, V_{ss2}^{M}, were determined as described in a previous work [23].

3. Results and discussion

When tyrosinase acts on M (tyrosine, Tyr), product formation (dopachrome, Cr) occurs after a lag period (τ, Fig. 1), from an initial steady-state to a final steady-state. The initial steady-state (Fig. 1 Inset) is defined by a rate, V_{ss1}^{Tyr}, tangential to the progress curve when $t \to 0$ (its determination was explained in a previous publication) [23]. At long times (Fig. 1), the system reaches the final steady-state characterised by the steady-state rate, V_{ss2}^{Tyr}.

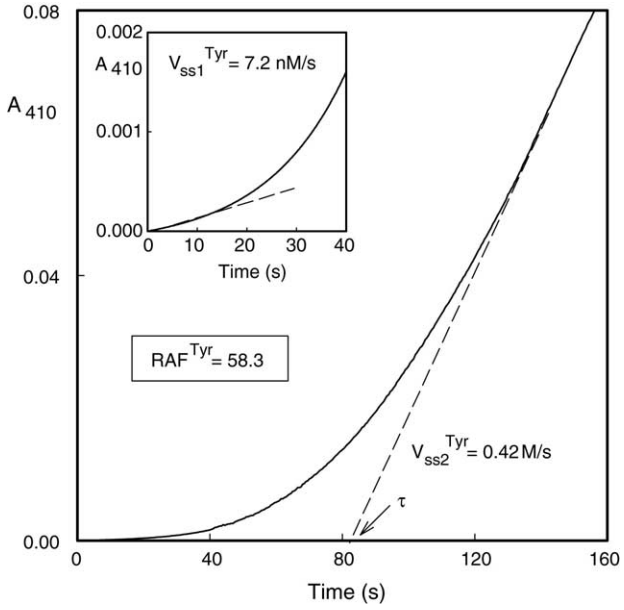

Fig. 1. Experimental recording of dopachrome formation from tyrosinase acting on L-tyrosine. The conditions were: 10 mM sodium phosphate buffer, pH 6.0, 0.54 mM L-tyrosine and 92 nM tyrosinase. (Inset) Experimental recordings at short times.

The experimental results for RAF^{Tyr} show a parabolic increase with respect to $[M]_0$ (Fig. 2). The same kinetic behaviour is observed in simulations of Mechanism I (Fig. 2). Whereas, simulations of Mechanism II point to values that

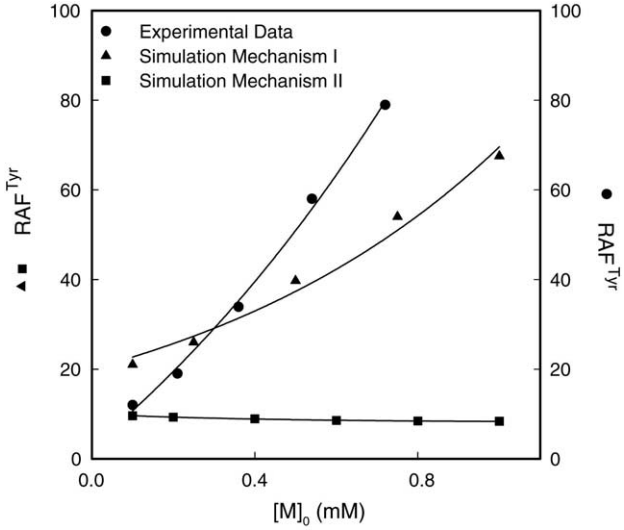

Fig. 2. Experimental data (●) and simulated data of the mechanisms of Scheme 1 (▲) and 2 (■) for the dependence of RAF^{Tyr} vs. $[M]_0$. The conditions were: (●) 10 mM sodium phosphate buffer, pH 6.0, L-tyrosine variation 0.09–0.72 mM; $[E]_0 = 170.53$ nM. (▲) $k_1 = 3.2 \times 10^5\ M^{-1}\ s^{-1}$, $k_{-1} = 10.8\ s^{-1}$, $k_2 = 3.8 \times 10^6\ M^{-1}\ s^{-1}$, $k_{-2} = 10\ s^{-1}$, $k_3 = 300\ s^{-1}$, $k_4 = 3.8 \times 10^4\ M^{-1}\ s^{-1}$, $k_{-4} = 10\ s^{-1}$, $k_{5_1} = 12\ s^{-1}$, $k_{5_2} = 24\ s^{-1}$, $k_6 = 3.8 \times 10^5\ M^{-1}\ s^{-1}$, $k_{-6} = 10\ s^{-1}$, $k_7 = 300\ s^{-1}$, $k_8 = 2.3 \times 10^7\ M^{-1}\ s^{-1}$, $k_{-8} = 1.07 \times 10^3\ s^{-1}$, $k_{app} = 1\ s^{-1}$, $[M]_0 = 0.1$–1 mM, $[E]_0 = 10$ nM, $[E_m] = 0.9\ [E]_0$, $[E_{ox}] = 0.1\ [E]_0$, $[O_2]_0 = 0.26$ mM. (■) The same conditions as (▲) but with $k_5 = 50\ s^{-1}$.

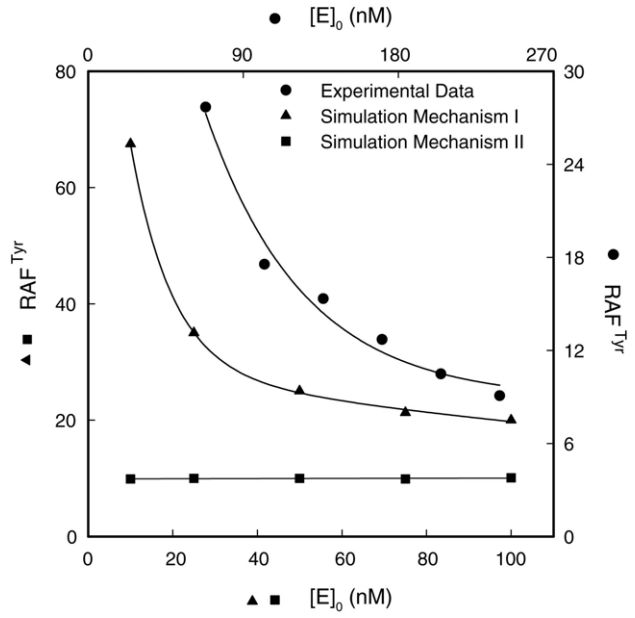

Fig. 3. Experimental data (●) and simulated data of the mechanisms of Scheme 1 (▲) and Scheme 2 (■) for the dependence of RAF^{Tyr} versus $[E]_0$. The conditions were: (●) 10 mM sodium phosphate buffer, pH 6.0, enzyme variation 68 to 238 nM; $[M]_0 = 0.18$ mM. (▲) The same conditions as Fig. 2 but with enzyme variation 10–100 nM and $[M]_0 = 1$ mM. (■) The same conditions as Fig. 2 but with enzyme variation 10–100 nM and $[M]_0 = 0.3$ mM.

are practically independent of $[M]_0$ (Fig. 2). Additionally, the experimental values of RAF^{Tyr} show a hyperbolic decrease with respect to $[E]_0$ (Fig. 3). The same dependence is observed in simulations of Mechanism I (Fig. 3), but not Mechanism II (Fig. 3).

3.1. Kinetic analysis: Mechanism II

The catalytic cycle proposed for monophenolase activity is (Scheme 2):

$$E_{ox} \overset{M}{\rightleftarrows} E_{ox}M \underset{Q}{\longrightarrow} E_d \overset{O_2}{\rightleftarrows} E_{ox} \tag{3}$$

The first steady-state would act with the proportion of E_{ox} existing in the native enzyme, for example it 10% of the total enzyme is in the oxy form $[E_{ox}]_{ss1} = [E_{ox}]_0 = 0.1[E]_0$. The quantity of E_{ox} during the second steady-state would be equal, at most, to the total enzyme available $[E_{ox}]_{ss2} = [E]_0$. Thus $[E_{ox}]_{ss2}$ would result from the conversion of E_m to E_{ox}. This would provide a maximum value of $RAF^{Tyr} = 10$, which would be constant for any range of $[E]_0$ (Fig. 3). Moreover, $RAF^{Tyr} \approx 10$ with any variation in $[M]_0$ (Fig. 2), since no transformation step $E_{ox}M \rightarrow E_mD$, no inhibition step $E_m + M \rightleftharpoons E_mM$ is considered (Scheme 2 versus Scheme 1).

Therefore, the erroneous structure of Mechanism II (Scheme 2) leads to the numerical simulations showing a kinetic behaviour different from that observed experimentally until 1999 [27], until 2003 [28] and with respect to the RAF^M data (Figs. 2 and 3).

3.2. Kinetic analysis: Mechanism I

The catalytic cycle proposed for the monophenolase activity is (Scheme 1):

$$E_{ox} \overset{M}{\rightleftarrows} E_{ox}M \rightarrow E_{ox} - M \rightarrow (E_mD)'$$
$$\rightarrow E_mD \underset{Q}{\longrightarrow} E_d \overset{O_2}{\rightleftarrows} E_{ox} \tag{4}$$

coupled to an inhibition pathway by M:

$$E_mD \overset{D}{\rightleftarrows} E_m \overset{M}{\rightleftarrows} E_mM \tag{5}$$

The E_mD intermediate divides between the catalytic cycle Eq. (4) and the inhibition pathway Eq. (5), controlled by the rate constants k_3, k_{-2}, $k_2[D]$ and $k_{5_2}[E_{ox} - M]$ (Scheme 1). We demonstrated [14] that in the oxidation stages of D to Q by E_m the enzymatic forms are not in rapid equilibrium, that is, $k_3 \geq k_{-2}$. At the start of the reaction $[M] = [M]_0$, $[D] = 0$, $k_3 \geq k_{-2}$ and $k_3 > k_{-2}$, $k_2[D]_{ss1}$ which cause the transformation of a portion of E_{ox} to the dead-end complex E_mM Eq. (5) after a series of turnovers with a burst of formation of Q Eq. (4) and the release of D Eq. (6):

$$E_{ox} \xrightarrow{M} E_{ox}M \rightarrow E_{ox} - M$$
$$\rightarrow (E_mD)' \rightarrow E_mD \underset{D}{\longrightarrow} E_m \xrightarrow{M} E_mM \tag{6}$$

The existence of this process Eq. (6) is supported by the release of D in similar amounts to $[E_{ox}]$ in the native enzyme, and thus $D_{released} \leq [E_{ox}]_0$, at the start of the monophenolase activity [3,24]. Later, from this situation $[D]_{ss1} = D_{released} \leq [E_{ox}]_0$, a *pseudo* steady-state is reached that satisfies $k_2[D]_{ss1} + k_{5_2}[E_{ox} - M] \simeq (k_3 + k_{-2})[E_mD]$. At the same time, an equilibrium is established in the inhibition pathway Eq. (5) permitting the entrance of a portion of $[E_mD] < [E_{ox}]_0$ in the catalytic cycle, which produces Q Eq. (4). As a consequence of the partition of $[E_{ox}]_0$ between catalysis and inhibition, the $[E_{ox}]$ available for the first steady-state of the enzyme $[E_{ox}]_{ss1}$, is considerably lower than the $[E_{ox}]$ present in the native enzyme $[E_{ox}]_0$. Thus, for example assuming that $[E_{ox}]_0 = 0.1[E]_0$, it is possible that the $[E_{ox}]$ available in the first steady-state is $[E_{ox}]_{ss1} = 0.1 \sim 1[E_{ox}]_0 = 0.01 \sim 0.1[E]_0$. The quantity of E_{ox} during the second steady-state would be $[E_{ox}]_{ss2} \gg [E_{ox}]$, $[E_{ox}]_{ss2} \simeq [E]_0$ due to the conversion of E_m to E_{ox} resulting from the increase of $[D]_{ss1}$ to $[D]_{ss2}$. Moreover, it has been shown that [14] the quantity of D in the second steady-state is:

$$[D]_{ss2} = \frac{k_{5_1}k_4(k_{-6} + k_7)}{2k_6k_7(k_{-4} + k_{5_1})}[M]_0 \tag{7}$$

This would provide values of $RAF^{Tyr} = 100$–10, similar to the experimental data obtained (Figs. 2 and 3). With the increase of $[M]_0$, the proportion of E_{ox} transformed to E_mM also increases Eq. (6), with the result that $[E_{ox}]_{ss1}$ decreases and

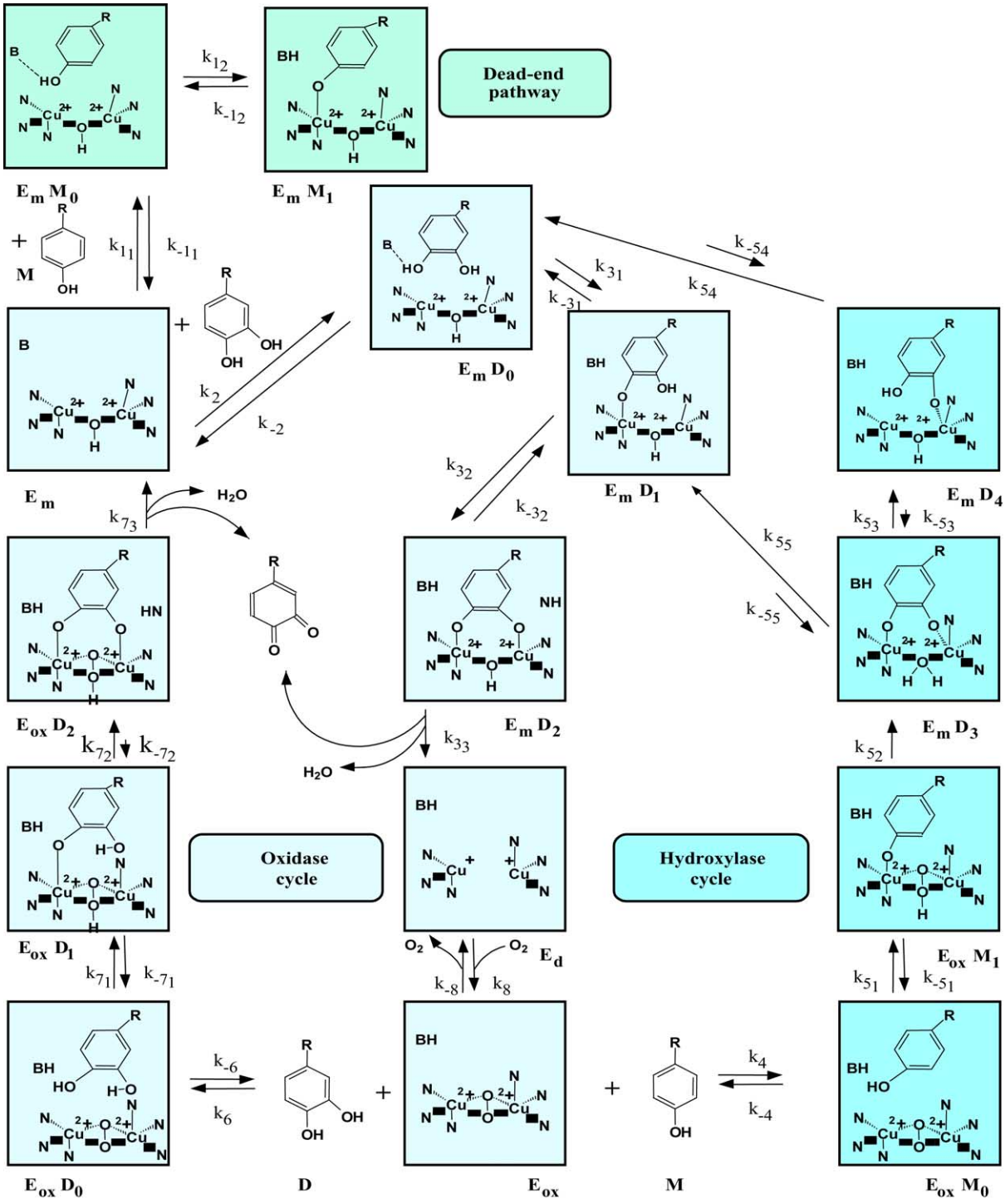

Scheme 3. Structural mechanism proposed to explain the kinetic reaction mechanism of tyrosinase acting on M. E_m, *met*tyrosinase; E_{ox}, *oxy*tyrosinase; E_d, *deoxy*tyrosinase; M, monophenol; D, *o*-diphenol; B, acid–base catalyst. *Dead-end pathway*: E_mM_0, interaction complex between E_m and *M*, E_mM_1, nucleophilic attack complex from *M* to E_m. *Oxidase cycle*: E_mD_0, interaction complex between E_m and *D*, E_mD_1, axial nucleophilic attack complex from OH of C-4 to E_m, E_mD_2, diaxial binding complex of *D* with E_m, $E_{ox}D_0$, interaction complex of *D* with E_{ox}, $E_{ox}D_1$, axial binding complex of *D* with E_{ox}, $E_{ox}D_2$ diaxial binding complex of *D* with E_{ox}. *Hydroxylase cycle*: $E_{ox}M_0$, interaction complex of *M* with E_{ox}, $E_{ox}M_1$, axial nucleophilic attack complex from *M* to E_{ox}, E_mD_3, axial-equatorial hydroxylation complex from *M* to *D*, E_mD_4, rearrangement complex with C-4 bond break.

RAF^M increases (Fig. 2). With the increase of $[E]_0$, $[E_{ox}]_0$ increases and this produces the release of more D to the medium and the increase of $[E_mD]$ (proportionally higher than $[E_mM]$). Thus, the first steady-state has more active enzyme (i.e. higher $[E_{ox}]_{ss1}$ and R_{ox1}) which implies lower autoactivation and RAF^M values (Fig. 3). Moreover, the experimentally observed behaviour of RAF^{Tyr} and the simulation of Mechanism I (Figs. 2 and 3) coincides with the results of the expression:

$$RAF^M = \frac{V^M_{ss2}}{V^M_{ss1}} = \frac{k^M_{cat2}K_1[M]_0 + k^M_{cat2}[M]^2_0}{\frac{k_3K_1}{2K_2}\left[K^M_{m2} + [M]_0\right][E]_0R_{ox1}}$$

$$= \frac{\alpha_1[M]_0 + \alpha_2[M]^2_0}{\left[\beta_1 + [M]_0\right][E]_0R_{ox1}} \quad (8)$$

where k^M_{cat2} is the catalytic constant for the second steady-state, K^M_{m2} is the Michaelis constant for the second steady-state, K_1 is the dissociation constant of E_mM complex ($K_2 = k_{-2}/k_2$), k_2 is the dissociation constant of E_mD complex ($k_2 = k_{-2}/k_2$) and $R_{ox1} = [E_{ox}]_{ss1}/[E]_0$. This equation is deduced from the analytical expressions of V^M_{ss1} and V^M_{ss2} previously reported Eqs. (1) and (5) [23]). The kinetic constants included in the α_1, α_2 and β_1 parameters have been described in the Appendix A.

3.3. Structural reaction mechanism

A possible structural interpretation of the kinetic reaction mechanism described in Scheme 1 is given in Scheme 3. The monophenolase catalytic cycle stages Eq. (4) and the inhibition pathway by M Eq. (5) are briefly described. Thus, the E_m form is attacked by the OH of C-4 of M, transferring its proton to the base (B) and producing an inactive dead-end complex, E_mM (Scheme 3). The E_{ox} form is active on M and is attacked by the OH of C-4 in an axial orientation, the proton being transferred to the peroxide [31]. Now, M is hydroxylated at the *ortho*-position by the electrophilic attack of the equatorially bound oxygen. To make itself accessible to such an attack M must turn, in order to generate D. During this step, the D produced is axially-equatorially bound and its molecular orbitals are not coplanar with the copper. It cannot therefore be oxidised in a concerted way and must reorientate itself to the oxidation position [43,44]. Tyrosinase does not carry out the oxidation of the phenol to a radical because it employs the (μ-η^2:η^2-peroxo)dicopper (II) intermediate to accomplish the aromatic oxygenation reaction of phenol, maintaining the distance of the copper atom at 3.5 Å. The enzyme can only accommodate the (μ-η^2:η^2-peroxo)dicopper (II) intermediate and not generate free radicals because it has a lower oxidation potential than the copper complex, bis(μ-oxo)dicopper (III), supported by the 2-(2-piridyl)ethylamine tridentate and bidentate ligands, which generate phenoxyl radical species with a phenol substrate [45]. This adjustment of the oxidation position may involve jumping from one of the coppers to the other and renewing the attack to achieve diaxial coplanarity. The intermediate bound to one copper only is more labile and so D can also free itself from the copper. This does in fact happen and its release has been demonstrated by GC–MS [24], an observation that supports the operation of the inhibition pathway of tyrosinase Eqs. (5) and (6).

3.4. Consequences of this reaction mechanism of tyrosinase

The lag period of the monophenolase activity whose origin is mainly due to the inhibition pathway by M with the enzymatic release of D Eqs. (4)–(6) is eliminated by the non-enzymatic accumulation of D formed from Q in the reaction medium (Scheme 1). The enzyme inhibition pathway by M acts as a brake on melanogenesis Eq. (6), since very little enzyme can act (E_{ox1}, Eq. (4), Fig. 1 inset). This delays the process until the non-enzymatic reactions from Q regenerate more D (Scheme 1), which recruit enzyme from the E_mM pool towards E_mD Eq. (5), Fig. 1, lag period) and a second steady-state is attained (Fig. 1). This originates a high autoactivation or increased rate from the initial to the final steady-state (RAF, Figs. 1–3), which can be explained by the corresponding analytical expressions Eq. (8). This paper, then, supports the reliability of the reaction mechanism proposed for tyrosinase (Scheme 1), as well as the correct pathway of melanogenesis Eq. (1) currently described in text books.

Acknowledgements

This work was supported in part by grants from the MCYT (Spain) Project AGL2002-01255 ALI, from the Fundación Séneca/Consejería de Agricultura, Agua y Medio Ambiente (Murcia) Project AGR/10/FS/02 and from the Fundación Séneca/Consejería de Educación y Universidades (Murcia) Project PI-79/00810/FS/01. LGF has a fellowship from the University of Murcia. FGM has a fellowship from the MEC (Spain).

Appendix A

$$\alpha_1 = \frac{4k_2k_{5_1}k_{5_2}k_4k_7(k_{-6}+k_7)K_1K_2}{[2k_{5_2}k_6k_7^2(3k_{-2}+k_3)(k_{-4}+k_{5_1}) + 2k_2k_3k_4k_7(k_{5_1}+k_{5_2})(k_{-6}+k_7)K_1 + k_2k_4k_{5_1}k_{5_2}(3k_7+k_3)(k_{-6}+k_7)K_1]}$$

$$\alpha_2 = \frac{4k_2k_{5_1}k_{5_2}k_4k_7(k_{-6}+k_7)K_2}{[2k_{5_2}k_6k_7^2(3k_{-2}+k_3)(k_{-4}+k_{5_1}) + 2k_2k_3k_4k_7(k_{5_1}+k_{5_2})(k_{-6}+k_7)K_1 + k_2k_4k_{5_1}k_{5_2}(3k_7+k_3)(k_{-6}+k_7)K_1]}$$

$$\beta_1 = \frac{2k_7k_{5_2}[k_6k_7(3k_{-2}+k_3)+k_2k_3(k_{-6}+k_7)](k_{-4}+k_{5_1})K_1}{[2k_{5_2}k_6k_7^2(3k_{-2}+k_3)(k_{-4}+k_{5_1})+2k_2k_3k_4k_7(k_{5_1}+k_{5_2})(k_{-6}+k_7)K_1+k_2k_4k_{5_1}k_{5_2}(3k_7+k_3)(k_{-6}+k_7)K_1]}$$

References

[1] H.S. Mason, Adv. Enzymol. 16 (1955) 105.
[2] G. Prota, M. d'Ischia, A. Napolitano, in: J.J. Nordlund, R. Boissy, V. Hearing, R. King, J.P. Ortonne (Eds.), The Pigmentary System, Univ. Press, Oxford, 1998.
[3] K. Lerch, in: H. Sigel (Ed.), Metal Ions in Biological Systems, Marcel Dekkler, New York, 1981.
[4] E.I. Solomon, U.M. Sundaram, T.E. Machonkin, Chem. Rev. 96 (1996) 2563.
[5] F. García-Carmona, F. García-Cánovas, J.L. Iborra, J.A. Lozano, Biochim. Biophys. Acta 717 (1982) 124.
[6] J.N. Rodríguez-López, J. Tudela, R. Varón, F. García-Cánovas, Biochim. Biophys. Acta 1076 (1991) 379.
[7] F. García-Cánovas, F. García-Carmona, J. Vera-Sánchez, J.L. Iborra, J.A. Lozano, J. Biol. Chem. 257 (1982) 8738.
[8] F. García-Carmona, J. Cabanes, F. García-Cánovas, Biochem. Int. 14 (1987) 1003.
[9] P. Serna, J.N. Rodríguez-López, J. Tudela, R. Varón, F. García-Cánovas, Biochem. J. 272 (1990) 459.
[10] F. García-Carmona, J. Cabanes, F. García-Cánovas, Biochim. Biophys. Acta 914 (1987) 198.
[11] J.N. Rodríguez-López, J. Escribano, F. García-Cánovas, Anal. Biochem. 216 (1994) 205.
[12] J. Cabanes, F. García-Cánovas, J.A. Lozano, F. García-Carmona, Biochim. Biophys. Acta 923 (1987) 187.
[13] J.N. Rodríguez-López, J. Tudela, R. Varón, F. García-Carmona, F. García-Cánovas, J. Biol. Chem. 267 (1992) 3801.
[14] J.R. Ros, J.N. Rodríguez-López, F. García-Cánovas, Biochim. Biophys. Acta 1204 (1994) 33.
[15] J.R. Ros, J.N. Rodríguez-López, F. García-Cánovas, Eur. J. Biochem. 222 (1994) 449.
[16] A. Sánchez-Ferrer, J.N. Rodríguez-López, F. García-Cánovas, F. García-Carmona, Biochim. Biophys. Acta 1247 (1995) 1.
[17] J.C. Espín, M. Morales, P.A. García-Ruiz, J. Tudela, F. García-Cánovas, J. Agric. Food Chem. 45 (1997) 1084.
[18] J.C. Espín, P.A. García-Ruiz, J. Tudela, R. Varón, F. García-Cánovas, J. Agric. Food Chem. 46 (1998) 968.
[19] J.C. Espín, P.A. García-Ruiz, J. Tudela, F. García-Cánovas, J. Agric. Food Chem. 46 (1998) 2469.
[20] J.C. Espín, P.A. García-Ruiz, J. Tudela, F. García-Cánovas, Biochem. J. 331 (1998) 547.
[21] J.N. Rodríguez-López, L.G. Fenoll, P.A. García-Ruiz, R. Varón, J. Tudela, R.N. Thorneley, F. Garcia-Canovas, Biochemistry 39 (2000) 10497.
[22] L.G. Fenoll, J.N. Rodríguez-López, J. García-Sevilla, J. Tudela, P.A. García-Ruiz, R. Varón, F. García-Cánovas, Eur. J. Biochem. 267 (2000) 5865.
[23] L.G. Fenoll, J.N. Rodríguez-López, J. García-Sevilla, P.A. García-Ruiz, R. Varón, F. García-Cánovas, J. Tudela, Biochim. Biophys. Acta 1548 (2001) 1.
[24] J.N. Rodríguez-López, L.G. Fenoll, M.J. Peñalver, P.A. García-Ruiz, R. Varón, F. Martínez-Ortiz, F. García-Cánovas, J. Tudela, Biochim. Biophys. Acta 1548 (2001) 238.
[25] C.J. Cooksey, P.J. Garratt, E.J. Land, S. Pavel, C.A. Ramsden, P.A. Riley, N.P.M. Smith, J. Biol. Chem. 272 (1997) 26226.
[26] P.A. Riley, J. Theor. Biol. 203 (2000) 1.
[27] J. Cabanes, S. Chazarra, F. García-Carmona, J. Theor. Biol. 214 (2002) 321.
[28] L.G. Fenoll, M.J. Peñalver, J.N. Rodríguez-López, R. Varón, F. García-Cánovas, J. Tudela, Int. J. Biochem. Cell Biol. 36 (2004) 235.
[29] L.G. Fenoll, J.N. Rodríguez-López, R. Varón, P.A. García-Ruiz, F. García-Cánovas, J. Tudela, Int. J. Biochem. Cell Biol. 34 (2002) 1594.
[30] M.J. Peñalver, A.N. Hiner, J.N. Rodríguez-López, F. García-Cánovas, J. Tudela, Biochim. Biophys. Acta 1597 (2002) 140.
[31] M.J. Peñalver, J.N. Rodríguez-López, P.A. García-Ruiz, F. García-Cánovas, J. Tudela, Biochim. Biophys. Acta 1650 (2003) 128.
[32] E.J. Land, C.A. Ramsden, P. Riley, Acc. Chem. Res. 36 (2003) 300.
[33] S.H. Pomerantz, J. Biol. Chem. 241 (1966) 161.
[34] H.W. Duckworth, J.E. Coleman, J. Biol. Chem. 245 (1970) 1613.
[35] M.M. Bradford, Anal. Biochem. 72 (1976) 248.
[36] J.N. Rodríguez-López, J.R. Ros, R. Varón, F. García-Cánovas, Biochem. J. 293 (1993) 859.
[37] R. Varón, B.H. Havsteen, M. García-Moreno, F. García-Cánovas, J. Tudela, Biochem. J. 270 (1990) 825.
[38] R. Varón, B.H. Havsteen, M. García-Moreno, F. García-Cánovas, J. Tudela, Biochem. J. 278 (1991) 91.
[39] J. Gálvez, R. Varón, J. Theor. Biol. 89 (1981) 1.
[40] C. Frieden, Methods Enzymol. 240 (1994) 311.
[41] C.F. Gerald, Applied Numerical Analysis, Addison-Wesley, Reading, 1978.
[42] F. García-Sevilla, C. Garrido del Solo, R.G. Duggleby, F. García-Cánovas, R. Peyro-García, R. Varón, BioSystems 54 (2000) 151.
[43] R.B. Woodward, R. Hoffmann, The Conservation of Orbital Symmetry, Academic Press, New York, 1970.
[44] T.L. Gilchrist, Storr organic reactions and orbital symmetry, Cambridge University Press, Cambridge, 1979.
[45] O. Takao, K. Ohkubo, M. Taki, Y. Tachi, S. Fukuzumi, S. Itoh, J. Am. Chem. Soc. 125 (2003) 11027.